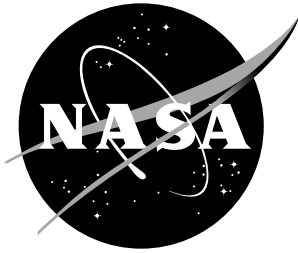


NASA/TM-1998-208699



Study of a Simulation Tool To Determine Achievable Control Dynamics and Control Power Requirements With Perfect Tracking

Aaron J. Ostroff
Langley Research Center, Hampton, Virginia

August 1998

The NASA STI Program Office ... in Profile

Since its founding, NASA has been dedicated to the advancement of aeronautics and space science. The NASA Scientific and Technical Information (STI) Program Office plays a key part in helping NASA maintain this important role.

The NASA STI Program Office is operated by Langley Research Center, the lead center for NASA's scientific and technical information. The NASA STI Program Office provides access to the NASA STI Database, the largest collection of aeronautical and space science STI in the world. The Program Office is also NASA's institutional mechanism for disseminating the results of its research and development activities. These results are published by NASA in the NASA STI Report Series, which includes the following report types:

- **TECHNICAL PUBLICATION.** Reports of completed research or a major significant phase of research that present the results of NASA programs and include extensive data or theoretical analysis. Includes compilations of significant scientific and technical data and information deemed to be of continuing reference value. NASA counter-part of peer reviewed formal professional papers, but having less stringent limitations on manuscript length and extent of graphic presentations.
- **TECHNICAL MEMORANDUM.** Scientific and technical findings that are preliminary or of specialized interest, e.g., quick release reports, working papers, and bibliographies that contain minimal annotation. Does not contain extensive analysis.
- **CONTRACTOR REPORT.** Scientific and technical findings by NASA-sponsored contractors and grantees.

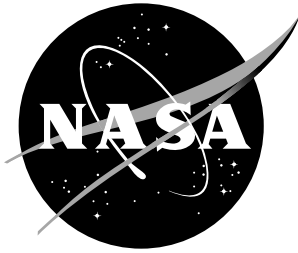
- **CONFERENCE PUBLICATION.** Collected papers from scientific and technical conferences, symposia, seminars, or other meetings sponsored or co-sponsored by NASA.
- **SPECIAL PUBLICATION.** Scientific, technical, or historical information from NASA programs, projects, and missions, often concerned with subjects having substantial public interest.
- **TECHNICAL TRANSLATION.** English-language translations of foreign scientific and technical material pertinent to NASA's mission.

Specialized services that help round out the STI Program Office's diverse offerings include creating custom thesauri, building customized databases, organizing and publishing research results ... even providing videos.

For more information about the NASA STI Program Office, see the following:

- Access the NASA STI Program Home Page at ***<http://www.sti.nasa.gov>***
- E-mail your question via the Internet to ***help@sti.nasa.gov***
- Fax your question to the NASA Access Help Desk at (301) 621-0134
- Phone the NASA Access Help Desk at (301) 621-0390
- Write to:
NASA Access Help Desk
NASA Center for AeroSpace Information
7121 Standard Drive
Hanover, MD 21076-1320

NASA/TM-1998-208699



Study of a Simulation Tool To Determine Achievable Control Dynamics and Control Power Requirements With Perfect Tracking

Aaron J. Ostroff
Langley Research Center, Hampton, Virginia

National Aeronautics and
Space Administration

Langley Research Center
Hampton, Virginia 23681-2199

August 1998

The use of trademarks or names of manufacturers in the report is for accurate reporting and does not constitute an official endorsement, either expressed or implied, of such products or manufacturers by the National Aeronautics and Space Administration.

Available from the following:

NASA Center for AeroSpace Information (CASI)
7121 Standard Drive
Hanover, MD 21076-1320
(301) 621-0390

National Technical Information Service (NTIS)
5285 Port Royal Road
Springfield, VA 22161-2171
(703) 487-4650

ABSTRACT

This paper contains a study of two methods for use in a generic nonlinear simulation tool that could be used to determine achievable control dynamics and control power requirements while performing perfect tracking maneuvers over the entire flight envelope. The two methods are NDI (nonlinear dynamic inversion) and the SOFFT (Stochastic Optimal Feedforward and Feedback Technology) feedforward control structure. Equivalent discrete and continuous SOFFT feedforward controllers have been developed. These equivalent forms clearly show that the closed-loop plant model loop is a plant inversion and is the same as the NDI formulation. The main difference is that the NDI formulation has a closed-loop controller structure whereas SOFFT uses an open-loop command model. Continuous, discrete, and hybrid controller structures have been developed and integrated into the formulation. Linear simulation results show that seven different configurations all give essentially the same response, with the NDI hybrid being slightly different. The SOFFT controller gave better tracking performance compared to the NDI controller when a nonlinear saturation element was added. Future plans include evaluation using a nonlinear simulation.

Introduction

There is a need within the aerospace community for a generic nonlinear piloted simulation tool that can be used to determine achievable control dynamics and control power requirements while it is performing perfect tracking maneuvers over the entire flight envelope. For this application the control law needs to be simple, and ideally it should be applicable to any aircraft without the need for adjustments. In addition, control law robustness should never be an issue. A simulation tool such as this would potentially have many applications within the control and general aerospace communities.

One application of this tool would allow a quick and easy comparison of various aerodynamic databases, while performing the same maneuvers. These databases could range from crude to high fidelity and could be used at various stages of development. This capability might be particularly important during evaluation of some of the novel control effector concepts presently being explored (ref. 1). A designer could adjust various parameters and evaluate force and moment capability relative to the entire aircraft database, and it could be done at various stages of development.

A second application could be the adjustment of flying qualities with pilot ratings while performing a variety of expected worst-case maneuvers. This application could help determine achievable dynamics and give the control designer guidelines for the best performance possible. Having this information, the designer could be more efficient while trying to improve performance. Another example is the development of guidelines for reconfigurable control systems to accommodate failures.

Control allocation configurations could also be evaluated since the control law is capable of perfect tracking, and the designer would not have to be concerned about the effect of control law deficiencies on the evaluation. A control allocation configuration must be selected a priori. For a given flying qualities model, various control allocation configurations can be compared, or vice-versa, for a given control allocation, various flying qualities models can be evaluated. With a selected flying qualities model and a

control allocation configuration, other variables such as stick shaping, deadband width, and stick gains could be evaluated.

It is likely that the large aerospace companies have a variety of tools available to accomplish the above objectives, although they may not have this specific tool. There is a need for smaller companies and government research organizations to have tools with the above capabilities to improve research efficiency.

A tool with the capability described was developed (ref. 2) by the Defence Research Agency (DRA) in the United Kingdom as part of a NASA/DRA Cooperative Aeronautical Research Program. The DRA called this exact nonlinear dynamic inversion (NDI) since the methodology is based upon dynamic inversion that was developed for flight control law design (ref. 3). The DRA application was to use the NDI as an analysis tool during simulation and extract moments and appropriate coefficients from the simulation. The ability to extract the appropriate terms from the simulation allows the control approach to be exact; therefore, control law robustness is not an issue.

The approach was successfully demonstrated on the HARV (High-Alpha Research Vehicle) (ref. 4) in the NASA Langley Differential Maneuvering Simulator. One deficiency with the reference 2 approach is that the incorporation of flying qualities was not developed. The control law only consisted of first- order responses, whereas military specifications (ref. 5) require higher-order responses.

To offset this deficiency, the SOFFT (Stochastic Optimal Feedforward and Feedback Technology) (refs. 6 and 7) methodology was investigated for applicability. SOFFT was developed for flight control application, and the feedforward structure allows precise tracking with the ability to incorporate any desired flying qualities into a command model which is imbedded within the feedforward controller. The approach was developed for a discrete controller by using linear models. Therefore, a disadvantage is that linear derivatives must be calculated in real time and then transformed to discrete form. The advantage over reference 2 is that higher order models can be used for exact tracking.

This paper contains a study of the two approaches for use in the development of a real-time piloted simulation tool which can be used to determine achievable control dynamics and control power requirements. The first section contains a review of the DRA approach to NDI. A review of the SOFFT approach is discussed in the second section and includes equations for both discrete and continuous controllers. Implementing SOFFT into a form similar to NDI shows that SOFFT also includes a plant inversion. The third section contains an analysis of the closed-loop plant model that illustrates the transfer function characteristics for both the continuous and discrete models. The fourth section shows an approach for incorporating flying qualities into the closed-loop NDI structure for both continuous formulations and discrete formulations. Hybrid formulations are then developed for both NDI and SOFFT. In the final section, simulation results illustrate that the methods give the same performance for purely linear plant models with all-continuous or all-discrete control systems. The hybrid SOFFT controller gave essentially the same results while the hybrid NDI controller had a slight error in the pitch rate response. In addition, the SOFFT structure gives better performance when a nonlinearity such as actuator saturation is included.

Symbols

A system matrix for continuous systems

a_f filter pole for plant inversion structure, rad/sec

a_{ij}	row i and column j element in A matrix
$A_V, A_\alpha, A_q, A_\theta$	row vectors in A_x (plant model) matrix
B_x	control input matrix for continuous systems
B_V, B_α, B_q	row vectors in B_x (plant model) matrix
C	output matrix for continuous systems
e	error signal
H_x, H_y	matrices used to select controlled states and outputs, respectively
I	identity matrix of appropriate dimensions
I_x, I_y, I_z	moments of inertia about the x-y-z axes, respectively
I_{xz}	xz axes product of inertia
K	gain for second-order continuous system response
K_u, K_z, K_x^*	matrices used in SOFFT feedforward controller
K_1, K_2, K_3	gains in the second-order discrete system response
L, M, N	roll, pitch, and yaw moments about the x-y-z axes, respectively
L_A, M_A, N_A	aerodynamic roll, pitch, and yaw moments, respectively
$L_{des}, M_{des}, N_{des}$	desired roll, pitch, and yaw moments, respectively
L_T, M_T, N_T	engine thrust roll, pitch, and yaw moments, respectively
L_x, M_x, N_x	airframe and engine roll, pitch, and yaw moments, respectively
$L_{\delta_{dir}}, N_{\delta_{dir}}$	roll and yaw moments for directional control
$L_{\delta_{lat}}, N_{\delta_{lat}}$	roll and yaw moments for lateral control
$M_{\delta_{lon}}$	pitch moment for longitudinal control
p, q, r	roll, pitch, and yaw rates about the x-y-z axes, respectively
$\dot{p}, \dot{q}, \dot{r}$	roll, pitch, and yaw accelerations about the x-y-z axes, respectively
s	Laplace transform variable
T	sampling period, sec

u	control signal
V	velocity
x	state-variable vector
\dot{x}	time derivative of state-variable vector
y	output-variable vector
z	z-transform variable
α	angle of attack
Γ	control matrix for discrete systems
γ_i	row i element in Γ matrix
$\delta_{dir}, \delta_{lat}, \delta_{lon}$	directional, lateral, and longitudinal control effectors, respectively
ζ	damping ratio
θ	pitch attitude
τ	time constant for first-order continuous system response
Φ	state transition matrix for discrete systems
ϕ_{ij}	row i and column j element in Φ matrix
ω	natural frequency for second-order continuous system response
ω_n	numerator frequency in second-order continuous system response

Subscripts:

des	desired command
k	coefficient for sampling sequence at time t_k
x	plant model
z	command model in SOFFT

Superscript:

*	attached to plant model to represent ideal variables
---	--

Abbreviations:

DRA	Defence Research Agency
FB	feedback controller
FF	feedforward controller
HARV	High-Alpha Research Vehicle
NDI	nonlinear dynamic inversion
SOFFT	Stochastic Optimal Feedforward and Feedback Technology

Review of Nonlinear Dynamic Inversion (NDI)

This section contains a review of the DRA approach to NDI, summarizing the key equations from reference 2. In this section, the x-y-z coordinate body axes are defined as shown in reference 8 with the x-axis out the nose, the y-axis positive in the direction of the right wing, and the z-axis down, completing a right-handed coordinate frame. The nonlinear moment equations (ref. 8) for a flat-earth, rigid-body, symmetrical airplane are

$$\begin{aligned}
 L_A + L_T &= I_x \dot{p} - I_{xz} \dot{r} - I_{xz} pq + (I_z - I_y) r q \\
 M_A + M_T &= I_y \dot{q} + (I_x - I_z) pr + I_{xz} (p^2 - r^2) \\
 N_A + N_T &= I_z \dot{r} - I_{xz} \dot{p} + (I_y - I_x) pq + I_{xz} qr
 \end{aligned} \tag{1}$$

where L_A , M_A , and N_A are the aerodynamic roll, pitch, and yaw moments about the x-y-z axes, respectively; L_T , M_T , and N_T are the moments about the x-y-z axes due to engine thrust; I_x , I_y , I_z , and I_{xz} are the moments and product of inertia; p , q , and r represent the roll, pitch, and yaw rates about the x-y-z axes; and \dot{p} , \dot{q} , and \dot{r} are the respective accelerations.

Moment data are usually defined in tables that are generated from wind tunnel and flight data. These tables usually contain coefficients that are nonlinear functions of many airplane variables, for example, angle-of-attack α , sideslip angle β , Mach, altitude h , and control surface deflections δ , and are denoted in a form such as

$$\begin{aligned}
 L &= L_x(\alpha, \beta, Mach, \dots) + L_{\delta_{lat}}(\alpha, \beta, Mach, \delta, \dots) \delta_{lat} + L_{\delta_{dir}}(\alpha, \beta, Mach, \delta, \dots) \delta_{dir} \\
 M &= M_x(\alpha, \beta, Mach, \dots) + M_{\delta_{lon}}(\alpha, \beta, Mach, \delta, \dots) \delta_{lon} \\
 N &= N_x(\alpha, \beta, Mach, \dots) + N_{\delta_{lat}}(\alpha, \beta, Mach, \delta, \dots) \delta_{lat} + N_{\delta_{dir}}(\alpha, \beta, Mach, \delta, \dots) \delta_{dir}
 \end{aligned} \tag{2}$$

For simplicity, the variables in parentheses will be represented by (...) in the remainder of this section. In equations (2), the nonlinear airframe and engine moment terms $L_x(\dots)$, $M_x(\dots)$, and $N_x(\dots)$ are shown separated from the nonlinear control moment effectiveness terms $L_{\delta_{lat}}(\dots)$, $L_{\delta_{dir}}(\dots)$, $M_{\delta_{lon}}(\dots)$, $N_{\delta_{lat}}(\dots)$, and $N_{\delta_{dir}}(\dots)$, which are shown multiplied by the control deflections (δ_{lat} , δ_{lon} , δ_{dir}). In actual practice, the moments may be a combination of several incremental moments generated within the simulation. In a linear problem, equations (2) would be

represented by linear derivatives multiplied by state variables and controls. Equations (2) assume one principal control about each of the three rotational axes. Control allocation methods, which are a separate problem, are required to distribute these control moments.

Desired acceleration commands, denoted by the subscript *des*, are generated by the controller. Rewriting equations (1) to reflect these desired commands and combining the aerodynamic and engine-generated moments yields

$$\begin{aligned} L_{des} &= I_x \dot{p}_{des} - I_{xz} \dot{r}_{des} - I_{xz} pq + (I_z - I_y)rq \\ M_{des} &= I_y \dot{q}_{des} + (I_x - I_z)pr + I_{xz}(p^2 - r^2) \\ N_{des} &= I_z \dot{r}_{des} - I_{xz} \dot{p}_{des} + (I_y - I_x)pq + I_{xz}qr \end{aligned} \quad (3)$$

which defines the required moments about each axis for any desired rotational acceleration. The required control deflections are calculated by rearranging equations (2) after substituting the desired moments for the left-hand sides. Separating the longitudinal and lateral-directional axes gives

$$\delta_{lon} = (M_{des} - M_x(\dots)) / M_{\delta_{lon}}(\dots) \quad (4)$$

$$\begin{Bmatrix} \delta_{lat} \\ \delta_{dir} \end{Bmatrix} = \begin{bmatrix} L_{\delta_{lat}}(\dots) & L_{\delta_{dir}}(\dots) \\ N_{\delta_{lat}}(\dots) & N_{\delta_{dir}}(\dots) \end{bmatrix}^{-1} \begin{Bmatrix} L_{des} - L_x(\dots) \\ N_{des} - N_x(\dots) \end{Bmatrix} \quad (5)$$

where the control effectiveness terms are inverted.

It is possible to bypass the control inversion and actuator models and pass moments directly to the simulation equations of motion in order to study control-power requirements. This configuration would effectively be a simulation with virtual moments. For example, $M_{des} - M_x(\dots)$ represents the longitudinal control moment required to make the aircraft respond perfectly to the desired moment. By using this operational mode, control allocation problems and actuator nonlinearities are avoided. During simulation, the required control power can be monitored for any desired flying qualities and maneuvers. For any maneuver in which peak control moments exceed available control moments, the excess required moments can be measured.

The above procedure can be summarized as

1. Create desired angular accelerations $\dot{p}_{des}, \dot{q}_{des}, \dot{r}_{des}$ from the Command Generator.
2. Implement eqs. (3) for $L_{des}, M_{des}, N_{des}$
3. Implement eqs. (4) and (5) to calculate $\delta_{lat}, \delta_{lon}, \delta_{dir}$

Outputs from the simulation include

1. Inertias I_x, I_y, I_z, I_{xz}
2. Airplane angular rates p, q, r
3. Aerodynamic and engine thrust moments $L_x(\dots), M_x(\dots), N_x(\dots)$

4. Control effectiveness terms $L_{\delta_{lat}}(\dots), L_{\delta_{dir}}(\dots), M_{\delta_{lon}}(\dots), N_{\delta_{lat}}(\dots), N_{\delta_{dir}}(\dots)$,

Figure 1 shows an example of the NDI procedure for a longitudinal case. The positive sign on the nonlinear dynamics terms is for consistency with the longitudinal expression in equations (3).

Review of the SOFFT Approach

SOFFT was developed (ref. 6) as a flight control methodology to separate the feedforward (FF) and feedback (FB) control objectives, in which each controller can be designed with different cost functions. The FF controller should be influenced mainly by objectives that relate system response to pilot input commands, whereas the FB controller should be influenced by objectives such as closed-loop stability, robustness, and noise attenuation. The SOFFT structure is shown in figure 2, where nominal trajectory commands y_x^* and u_x^* are calculated by the FF controller and then sent to the FB controller and plant input, respectively. Errors in the FF signals are then compensated for by the feedback controller.

Since the objective of this paper is to investigate a technique that can perform perfect tracking during simulation, only the SOFFT FF part of the control methodology needs to be explored. As shown in figure 3, the SOFFT FF controller consists of a command model, a plant model, and FF gains. All SOFFT dynamics are in discrete form, and the subscript k represents the sampling sequence at time t_k .

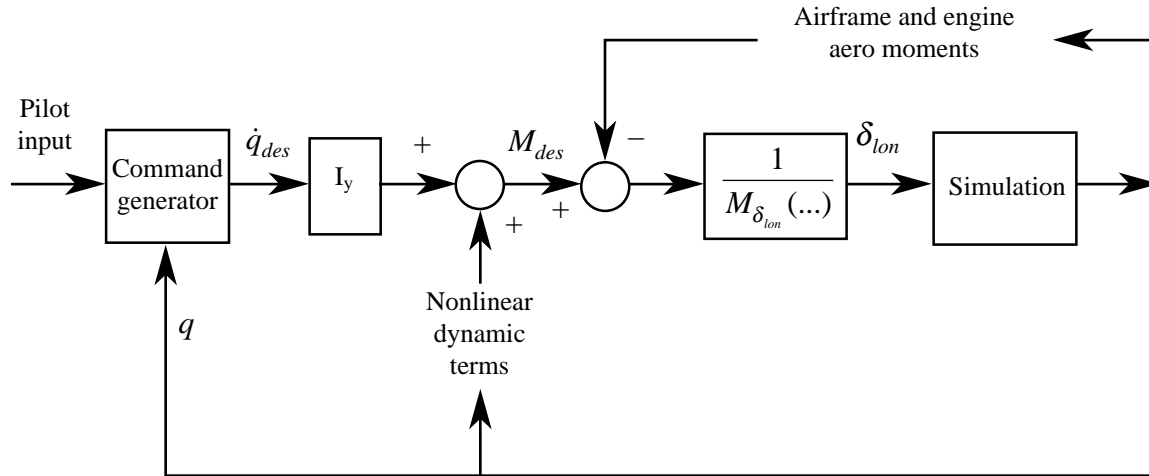


Figure 1. Longitudinal example of NDI approach.

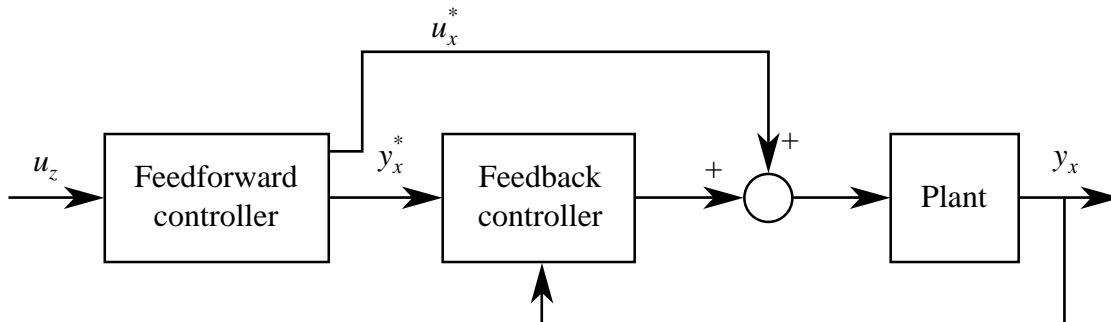


Figure 2. SOFFT control system structure.

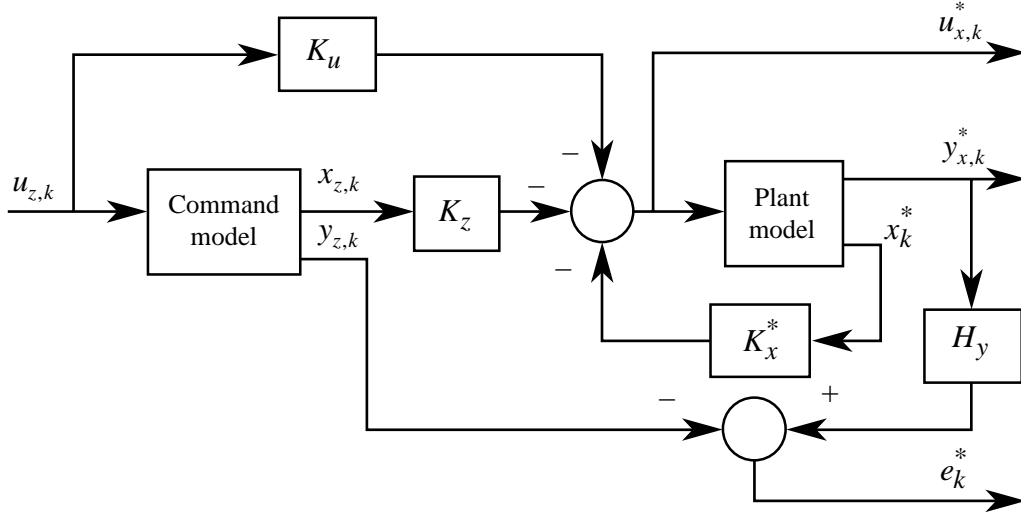


Figure 3. SOFFT feedforward controller structure.

The command model incorporates flying qualities dynamics and transforms the input vector $u_{z,k}$, representative of pilot commands, into a commanded state vector $x_{z,k}$ and its corresponding output vector $y_{z,k}$. The difference between pilot stick input and $u_{z,k}$ would typically include stick gains, stick shaping, and possibly a small deadband. A calculated control signal vector $u_{x,k}^*$ is input to the plant model that contains discrete dynamics representative of the actual plant. Outputs from the plant model are the state vector x_k^* , which is fed back to the plant model input and the corresponding output vector $y_{x,k}^*$. Feedforward (FF) controller gain matrices K_u , K_z , and K_x^* are based upon making selected plant model outputs (or combinations of outputs), defined by constant matrix H_y , precisely track command model outputs. With perfect plant model tracking, the error vector signal e_k^* is always zero. When this concept is used, the FF controller will always have perfect tracking for whatever plant model is being used.

Discrete Modeling

Discrete dynamic equations describing the plant model and command model are

$$\begin{aligned} x_{k+1}^* &= \Phi_x x_k^* + \Gamma_x u_{x,k}^* \\ y_{x,k}^* &= C_x x_k^* \end{aligned} \quad (6)$$

$$\begin{aligned} x_{z,k+1} &= \Phi_z x_{z,k} + \Gamma_z u_{z,k} \\ y_{z,k} &= C_z x_{z,k} \end{aligned} \quad (7)$$

where subscripts x and z represent the plant model and command model, respectively, Φ represents a discrete state transition matrix, Γ represents a discrete control matrix, and C represents the output matrix. Perfect tracking is accomplished when

$$e_k^* = H_y y_{x,k}^* - y_{z,k} = 0. \quad (8)$$

Define H_x by

$$H_y y_{x,k}^* = H_y C_x x_k^* = H_x x_k^* \quad (9)$$

such that $H_x = H_y C_x$.

The FF gain matrices are calculated based upon equation (8) as (ref. 6):

$$K_u = -[H_x \Gamma_x]^{-1} C_z \Gamma_z \quad (10)$$

$$K_z = -[H_x \Gamma_x]^{-1} C_z \Phi_z \quad (11)$$

$$K_x^* = [H_x \Gamma_x]^{-1} H_x \Phi_x \quad (12)$$

An equivalent SOFFT feedforward controller structure can be developed by inserting the FF gains into the control equation

$$u_{x,k}^* = -K_u u_{z,k} - K_z x_{z,k} - K_x^* x_k^* \quad (13)$$

and after factoring out the control inverse term $[H_x \Gamma_x]^{-1}$ and using equations (6) and (7) yields

$$u_{x,k}^* = [H_x \Gamma_x]^{-1} \{y_{z,k+1} - H_x \Phi_x x_k^*\}. \quad (14)$$

This equivalent SOFFT feedforward control structure is illustrated in figure 4. Clearly one advantage of this form over the form shown in figure 3 is that gain matrices K_u and K_z do not have to be explicitly

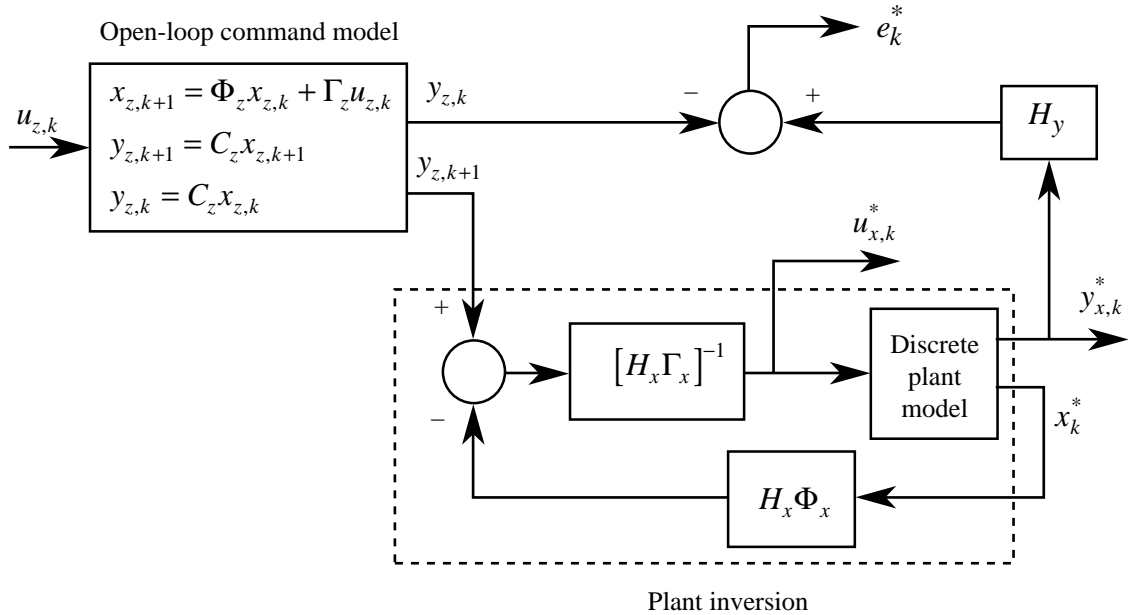


Figure 4. Equivalent SOFFT discrete feedforward controller structure.

calculated. The closed-loop plant model shown within the dashed box represents a plant inversion for the controlled variables, with inputs clearly coming from an open-loop command model. The approach to calculate moments as in the NDI approach will be discussed after the next section on continuous modeling.

Continuous Modeling

Although SOFFT was developed by using a discrete form, similar equations can be developed for continuous plant and command models. Dynamic equations for the continuous plant model and command model are

$$\begin{aligned}\dot{x}^* &= A_x x^* + B_x u_x^* \\ y_x^* &= C_x x^*\end{aligned}\tag{15}$$

$$\begin{aligned}\dot{x}_z &= A_z x_z + B_z u_z \\ y_z &= C_z x_z\end{aligned}\tag{16}$$

where A represents the state transition matrix, B represents the control matrix, C represents the output matrix, and the subscripts are the same as defined previously. Perfect tracking is accomplished when

$$e^* = H_y y_x^* - y_z = 0\tag{17}$$

Defining the FF gain matrices as

$$K_u = -[H_x B_x]^{-1} C_z B_z\tag{18}$$

$$K_z = -[H_x B_x]^{-1} C_z A_z\tag{19}$$

$$K_x^* = [H_x B_x]^{-1} H_x A_x\tag{20}$$

and inserting these gain matrices into the control equation gives

$$u_x^* = [H_x B_x]^{-1} \left\{ \dot{y}_z - H_x A_x x^* \right\}\tag{21}$$

The equivalent form for the continuous SOFFT feedforward controller is shown in figure 5. Again, the closed-loop plant model shown within the dashed box represents a plant inversion. In the following section it will be shown that the transfer function of the continuous model is different from the transfer function of the discrete model.

Incorporating inertia terms into the controller in figure 5 creates a closed-loop plant model that can be shown to have effectively an equivalent portion in figure 1. The nonlinear dynamics terms are not included in figure 5. Using the longitudinal example and multiplying \dot{y}_z (which corresponds to \dot{q}_{des} in figure 1) by I_y gives a moment command. Multiplying the plant model feedback by I_y is the same as feeding back the plant aerodynamic moments, and incorporating the inverse of I_y into the plant input path gives the inverse of the control effectiveness term in figure 1.

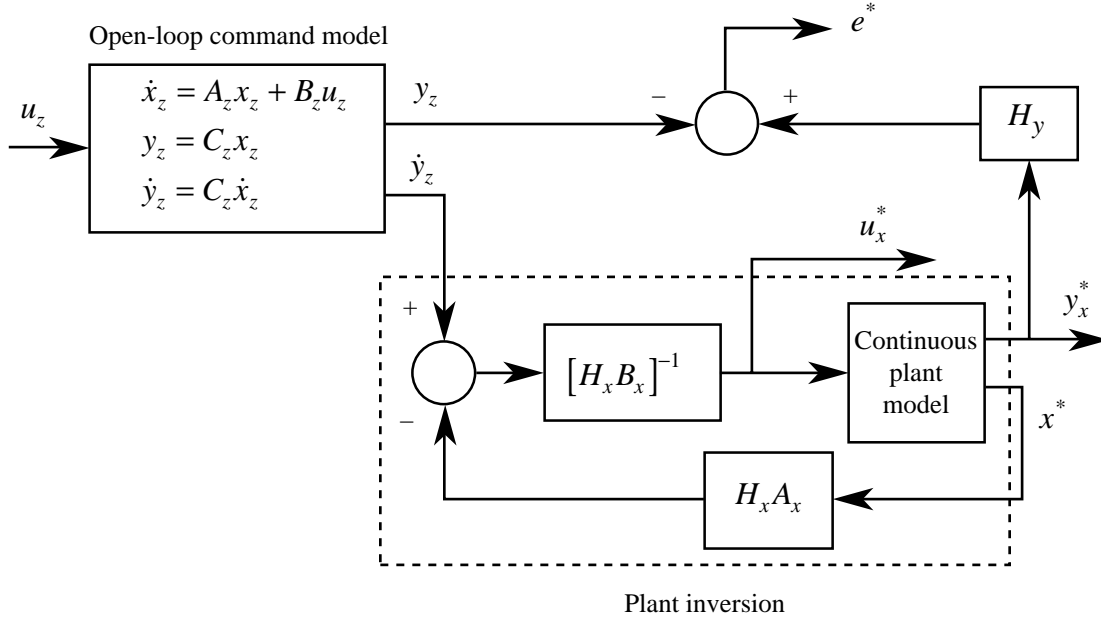


Figure 5. Equivalent SOFFT continuous feedforward controller structure.

Moments can also be generated in the discrete controller in figure 4, but the approach is more complicated. A moment command can be generated by taking the time increment $y_{z,k+1} - y_{z,k}$, which is then multiplied by I_y / T , where T is the sampling period. Similar increments must be created in the plant feedback path and the plant input path.

Closed-Loop Analysis

This section contains an analysis of the closed-loop plant model and illustrates the transfer function characteristics for both the continuous model and the discrete model. It should be noted that a nonminimum phase system will result in an unstable closed-loop system for any configuration since the zeros of the open-loop plant become poles of the closed-loop plant model.

The continuous model transfer function is illustrated first using a longitudinal example. Let

$$x^* = [V, \alpha, q, \theta]^T \quad (22)$$

where V is the total velocity, α is the angle of attack, q is the pitch rate, and θ is the pitch attitude. The A_x matrix is defined in terms of row vectors, and the B_x matrix is defined in terms of scalar elements as

$$A_x = \begin{bmatrix} A_V \\ A_\alpha \\ A_q \\ A_\theta \end{bmatrix} \quad \text{and} \quad B_x = \begin{bmatrix} B_V \\ B_\alpha \\ B_q \\ 0 \end{bmatrix} \quad (23)$$

since there is one control for this example. Assuming a pitch rate command with the plant model output matrix C_x an identity matrix, then H_x and H_y are identical from the definition in equation (9) as

$$H_x = H_y = [0 \ 0 \ 1 \ 0] \quad (24)$$

giving

$$\begin{aligned} H_x A_x &= A_q \\ H_x B_x &= B_q \end{aligned} \quad (25)$$

Inserting equations (25) into (21) and then the combination into equations (15) and making use of the definition in equation (9) gives

$$\begin{aligned} \dot{x}^* &= \begin{bmatrix} A_V - B_V B_q^{-1} A_q \\ A_\alpha - B_\alpha B_q^{-1} A_q \\ 0 \\ A_\theta \end{bmatrix} x^* + \begin{bmatrix} B_V B_q^{-1} \\ B_\alpha B_q^{-1} \\ 1 \\ 0 \end{bmatrix} \dot{y}_z \\ H_y y_x^* &= H_y C_x x^* = H_x x^* \end{aligned} \quad (26)$$

showing that the transfer function from \dot{y}_z to $H_x y_x^*$ is an integrator, as illustrated in figure 6. Notice that the internal dynamics for the uncontrolled states will be modified from their open-loop characteristics.

If the controlled variable is a linear combination of states where, for example, H_x and H_y are defined as

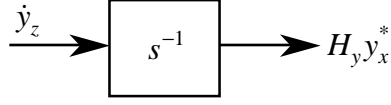
$$H_x = H_y = [0 \ 0.1 \ 1 \ 0] \quad (27)$$

then the system and control input matrices in equation (26) will be modified as

$$\begin{aligned} \dot{x}^* &= \begin{bmatrix} A_V - B_V \frac{0.1A_\alpha + A_q}{0.1B_\alpha + B_q} \\ A_\alpha - B_\alpha \frac{0.1A_\alpha + A_q}{0.1B_\alpha + B_q} \\ A_q - B_q \frac{0.1A_\alpha + A_q}{0.1B_\alpha + B_q} \\ A_\theta \end{bmatrix} x^* + \begin{bmatrix} \frac{B_V}{0.1B_\alpha + B_q} \\ \frac{B_\alpha}{0.1B_\alpha + B_q} \\ \frac{B_q}{0.1B_\alpha + B_q} \\ 0 \end{bmatrix} \dot{y}_z \\ H_y y_x^* &= H_y C_x x^* = H_x x^* \end{aligned} \quad (28)$$

Similar to the previous example, the transfer function from \dot{y}_z to $H_x y_x^*$ is an integrator. This integration can be easily seen by premultiplying the \dot{x}^* equation by H_x . The resulting system matrix will be $\mathbf{0}$ and the resulting control input will be scalar and equal to 1.

Continuous closed-loop plant model



Discrete closed-loop plant model

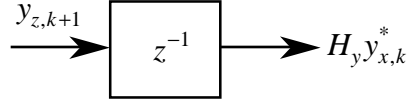


Figure 6. Transfer functions for continuous and discrete closed-loop plant models.

A similar analysis can be made for a discrete system by making use of equation (14) for $u_{x,k}^*$. Given the same pitch rate command defined in equation (24), the dynamic equations for the FF controller become

$$x_{k+1}^* = \begin{bmatrix} \Phi_V - \Gamma_V \Gamma_q^{-1} \Phi_q \\ \Phi_\alpha - \Gamma_\alpha \Gamma_q^{-1} \Phi_q \\ 0 \\ \Phi_\theta \end{bmatrix} x_k^* + \begin{bmatrix} \Gamma_V \Gamma_q^{-1} \\ \Gamma_\alpha \Gamma_q^{-1} \\ 1 \\ \Gamma_\theta \Gamma_q^{-1} \end{bmatrix} y_{z,k+1} \quad (29)$$

$$H_y y_{x,k}^* = H_x x_k^*$$

where again C_x is an identity matrix. The main point of equation (29) is that the transfer function for the controlled variables in a discrete system is not an integrator, but is a time delay as illustrated in figure 6.

Other Configurations

It is possible to create a system matrix for continuous systems or a state transition matrix for discrete systems with nonzero elements in the controlled channel. For example, a first-order filter can be developed by modifying the feedback in figure 5 to be $H_x(A_x + a_f I)$ where a_f is the filter frequency and I is an appropriate identity matrix. By using this feedback, the pitch rate closed-loop system in equation (26) is modified as

$$\dot{x}^* = \begin{bmatrix} A_V - B_V B_q^{-1} (A_q + a_f) \\ A_\alpha - B_\alpha B_q^{-1} (A_q + a_f) \\ -a_f \\ A_\theta \end{bmatrix} x^* + \begin{bmatrix} B_V B_q^{-1} \\ B_\alpha B_q^{-1} \\ 1 \\ 0 \end{bmatrix} a_f y_z \quad (30)$$

$$H_y y_x^* = H_y C_x x^* = H_x x^*$$

where the filter frequency is the only element in the modified system matrix. Since a low-pass filter is created, the input should be the commanded response y_z rather than the first derivative, which is needed when an integrator is formed. The input is shown multiplied by a_f to create a unity-gain filter. This modified feedback will be shown in a later section for development of a SOFFT hybrid controller. A

linear combination of states, as illustrated in equation (28), can also be implemented for the filter approach.

Discrete systems can be modified in a similar manner. For example, a discrete integrator can be implemented by feeding back $H_x(\Phi_x - I)$ in place of $H_x\Phi_x$ in figure 4. This revised feedback will create a “1” in the modified system matrix replacing the “0” in equation (29).

The next section will show how to implement closed-loop controllers for all continuous models, for all discrete models, and for two hybrid cases where the plant is continuous but the controller is a sample data system. The hybrid system is expected to be the case for the desired application.

Incorporation of Flying Qualities

This section shows how command models can be integrated with the closed-loop plant inversion transfer function to get the NDI form illustrated in figure 1. First- and second-order models are shown for continuous, discrete, and hybrid controllers. These models can be used either as open-loop command models for use in SOFFT (figs. 4 and 5) or as closed-loop integrated models as in NDI. In this section, subscript “c” is used for the input command.

First-Order Continuous Formulation

Suppose a first-order transfer function with time constant τ of the form shown below is desired,

$$\frac{y}{u_c}(s) = \frac{1}{\tau s + 1} = \frac{1/\tau}{s + 1/\tau} \quad (31)$$

then the problem is to transform equation (31) into a form that uses the integrator characteristic of the closed-loop plant inversion model. The modeling approach used is to cross multiply as

$$\left(s + \frac{1}{\tau}\right)y(s) = \frac{1}{\tau}u_c(s) \quad (32)$$

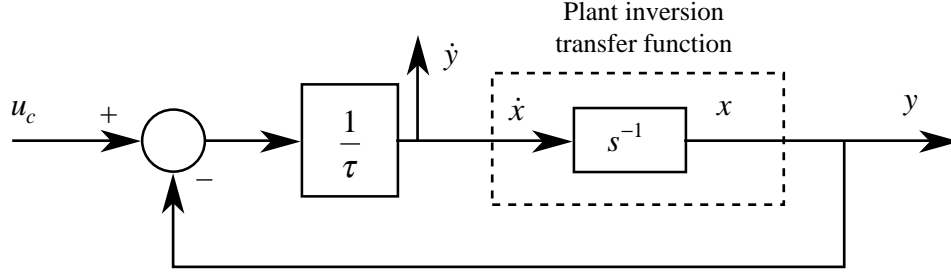
then solve for $y(s)$ as

$$y(s) = \frac{1}{\tau} s^{-1} \{u_c(s) - y(s)\} \quad (33)$$

which is implemented as a closed-loop controller, as shown in figure 7. The plant inversion transfer function described in the previous section is illustrated by the dashed box when $y = x$. Implementation of the first-order controller does not require any dynamic elements.

The state-space transfer function is given as

$$\begin{aligned} \dot{x} &= -\frac{1}{\tau}x + \frac{1}{\tau}u_c \\ y &= x \\ \dot{y} &= -\frac{1}{\tau}x + \frac{1}{\tau}u_c \end{aligned} \quad (34)$$



$$\frac{y}{u_c}(s) = \frac{1/\tau}{s + 1/\tau}$$

Figure 7. First-order transfer function for continuous models.

where equation (34) can be used as the SOFFT continuous open-loop command model shown in figure 5.

Second-Order Continuous Formulation

The first-order transfer function was trivial and could have been implemented directly from equation (31). The next case is for a second-order transfer function with numerator dynamics such as

$$\frac{y}{u_c}(s) = \frac{K(s + \omega_n)}{s^2 + 2\zeta\omega s + \omega^2} \quad (35)$$

where ω is the natural frequency, ζ is the damping ratio, and ω_n is a zero of the transfer function. Using the approach shown above gives

$$(s^2 + 2\zeta\omega s + \omega^2)y(s) = K(s + \omega_n)u_c(s) \quad (36)$$

and after combining terms with powers of s , the equation to be programmed for $y(s)$ is

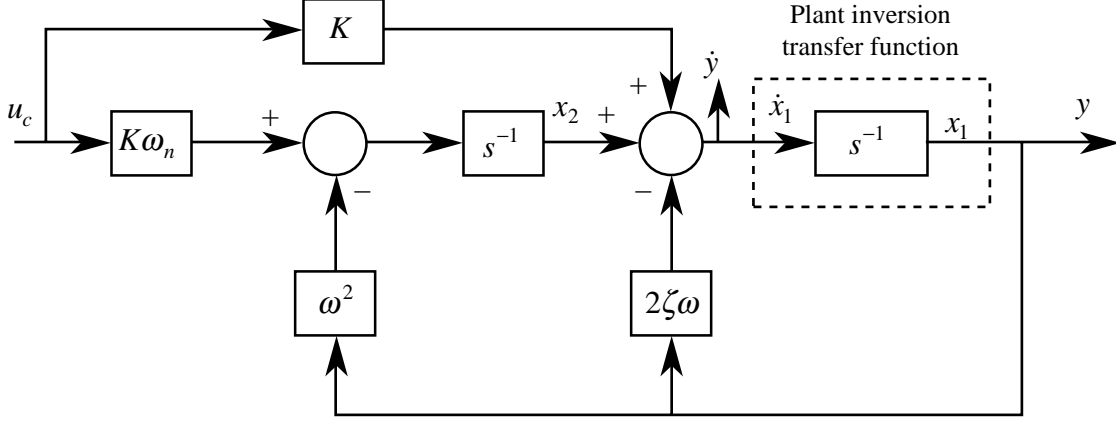
$$y(s) = s^{-1}\{Ku_c(s) - 2\zeta\omega y(s)\} + s^{-2}\{K\omega_n u_c(s) - \omega^2 y(s)\} \quad (37)$$

which is implemented as a closed-loop controller, as shown in figure 8.

The state-space transfer function for this model is given as

$$\begin{aligned} \begin{bmatrix} \dot{x}_1 \\ \dot{x}_2 \end{bmatrix} &= \begin{bmatrix} -2\zeta\omega & 1 \\ -\omega^2 & 0 \end{bmatrix} \begin{bmatrix} x_1 \\ x_2 \end{bmatrix} + \begin{bmatrix} K \\ K\omega_n \end{bmatrix} u_c \\ \begin{bmatrix} y \\ \dot{y} \end{bmatrix} &= \begin{bmatrix} 1 & 0 \\ -2\zeta\omega & 1 \end{bmatrix} \begin{bmatrix} x_1 \\ x_2 \end{bmatrix} + \begin{bmatrix} 0 \\ K \end{bmatrix} u_c \end{aligned} \quad (38)$$

which can be used as the SOFFT continuous open-loop command model shown in figure 5.



$$\frac{y}{u_c}(s) = \frac{K(s + \omega_n)}{s^2 + 2\zeta\omega s + \omega^2}$$

Figure 8. Second-order transfer function for continuous models.

First-Order Discrete Formulation

For the application being investigated in this paper, an all-discrete simulation is unlikely since variables extracted from the simulation are expected to be in continuous form. The desired approach is to extract variables directly from the nonlinear simulation, if possible. Another possible approach is to create linear models during each iteration and, if this is the case, these linear models could then be discretized. Furthermore, for a FF flight controller application, an all discrete formulation is a viable candidate. For these reasons and since this methodology is closely aligned to the continuous formulation, the approach is included.

The discrete state-space representation for a dynamic system is

$$\begin{aligned} x_{k+1} &= \Phi x_k + \Gamma u_{c,k} \\ y_k &= x_k \\ y_{k+1} &= \Phi x_k + \Gamma u_{c,k} \end{aligned} \quad (39)$$

which is illustrated in figure 9. Typically, the designer specifies a transfer function of the form shown in equation (31) or the equivalent state-space form shown in equation (34), which must then be transformed to the discrete plane. The equations for Φ and Γ are approximated by the series expansion

$$\begin{aligned} \Phi &= e^{AT} \approx 1 - \frac{T}{\tau} + \frac{1}{2} \left(\frac{T}{\tau} \right)^2 - \frac{1}{6} \left(\frac{T}{\tau} \right)^3 + \dots \\ \Gamma &= A^{-1} [\Phi - I] B \approx \frac{T}{\tau} \left[1 - \frac{1}{2} \frac{T}{\tau} + \frac{1}{6} \left(\frac{T}{\tau} \right)^2 - \dots \right] \end{aligned} \quad (40)$$

where a third-order expansion is used above. A third-order expansion is practical for a flight controller with sampling rates of 40 to 80 Hz. Since the plant model is discrete, the plant inversion transfer

function, shown in the dashed box of figure 9, is represented as a time delay, as discussed previously. The closed-loop NDI controller does not have any dynamic elements in the implementation. Equations (39) are used as the SOFFT open-loop command model in figure 4.

Second-Order Discrete Formulation

Starting with the continuous state-space model in equations (38), the four components of Φ and two components of Γ can be expanded as

$$\begin{aligned}\phi_{11} &\approx 1 + a_{11}T + \frac{T^2}{2}(a_{11}^2 + a_{21}) + \frac{T^3}{6}(a_{11}^3 + 2a_{11}a_{21}) + \dots \\ \phi_{12} &\approx T[\frac{T}{2}a_{11} + \frac{T^2}{6}(a_{11}^2 + a_{21}) + \dots] \\ \phi_{21} &\approx T[a_{21} + \frac{T}{2}a_{11}a_{21} + \frac{T^2}{6}(a_{11}^2a_{21} + a_{21}^2) + \dots] \\ \phi_{22} &\approx 1 + \frac{T^2}{2}a_{21} + \frac{T^3}{6}a_{11}a_{21} + \dots\end{aligned}\tag{41}$$

$$\begin{aligned}\gamma_1 &\approx \frac{K}{a_{21}}(\phi_{21} + b_2\phi_{22} - b_2) \\ \gamma_2 &\approx K(\phi_{11} - 1 + b_2\phi_{12}) - a_{11}\gamma_1\end{aligned}\tag{42}$$

where the subscripts represent row and column designation. These equations can then be implemented by transforming equations (39) into the form

$$\begin{aligned}x(z) &= [zI - \Phi]^{-1}\Gamma u_c(z) \\ y(z) &= [1 \quad 0]x(z) = x_1(z)\end{aligned}\tag{43}$$

and for the second-order discrete system the solution for $y(z)$ is

$$y(z) = \frac{[z\gamma_1 + K_1]}{z^2 + K_3z + K_2}u_c(z)\tag{44}$$

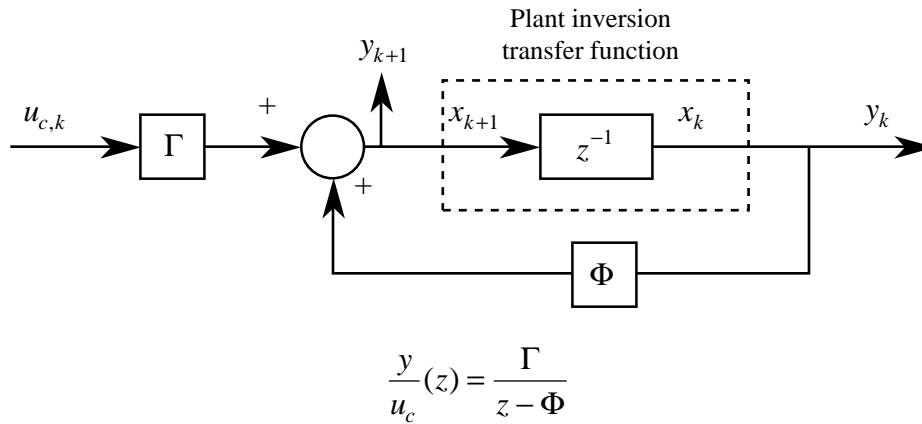


Figure 9. First-order transfer function for discrete models.

where

$$\begin{aligned} K_1 &= \gamma_2 \phi_{12} - \gamma_1 \phi_{22} \\ K_2 &= \phi_{11} \phi_{22} - \phi_{12} \phi_{21} \\ K_3 &= -(\phi_{11} + \phi_{22}) \end{aligned} \quad (45)$$

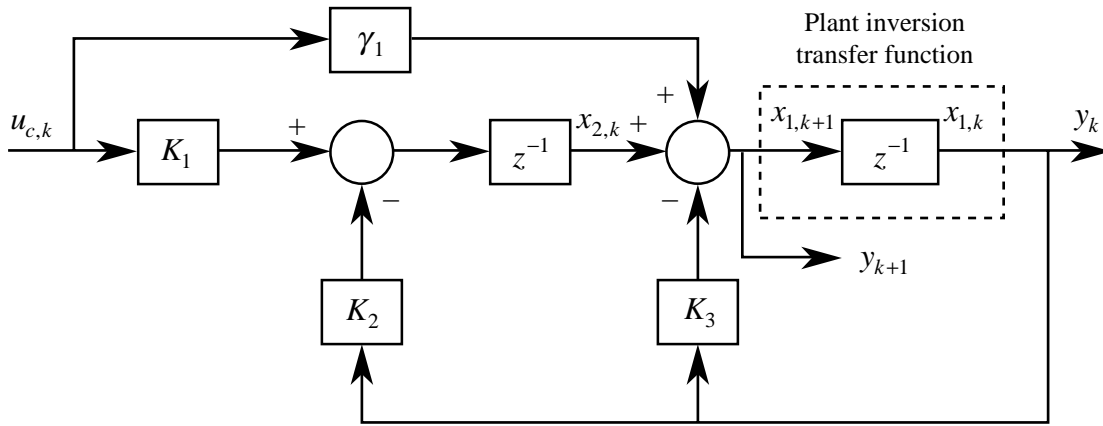
Figure 10 contains the diagram for the second-order discrete model. For the NDI implementation, the controller only requires one dynamic element.

The state-space representation for figure 10 is

$$\begin{aligned} \begin{Bmatrix} x_{1,k+1} \\ x_{2,k+1} \end{Bmatrix} &= \begin{bmatrix} -K_3 & 1 \\ -K_2 & 0 \end{bmatrix} \begin{Bmatrix} x_{1,k} \\ x_{2,k} \end{Bmatrix} + \begin{bmatrix} \gamma_1 \\ K_1 \end{bmatrix} u_{c,k} \\ \begin{Bmatrix} y_k \\ y_{k+1} \end{Bmatrix} &= \begin{bmatrix} 1 & 0 \\ -K_3 & 1 \end{bmatrix} \begin{Bmatrix} x_{1,k} \\ x_{2,k} \end{Bmatrix} + \begin{bmatrix} 0 \\ \gamma_1 \end{bmatrix} u_{c,k} \end{aligned} \quad (46)$$

which is the same form as the original continuous state-space equations (38), but with transformed elements. Equations (46) would be implemented in figure 4 for the SOFFT open-loop command model.

If a discrete integrator implementation is used for the plant inversion process by feeding back $H_x(\Phi_x - I)$ in place of $H_x \Phi_x$ in figure 4, then a SOFFT open-loop incremental model would be used. The incremental command into the plant inversion is $(y_{z,k+1} - y_{z,k})$. Moments can easily be generated in this linear implementation by multiplying the incremental command and the plant feedback by the inertia normalized by the sampling period (I_y / T for the longitudinal example) and dividing the control input by this same factor.



$$\frac{y}{u_c}(z) = \frac{z\gamma_1 + K_1}{z^2 + K_3z + K_2}$$

Figure 10. Second-order transfer function for discrete models.

Hybrid Controllers

The typical situation for the application defined in this paper is to have a combination of a continuous plant and a sampled data controller that contains discrete dynamic elements. The plant would appear to be continuous since numerical integration will be used for the equations of motion, and variables extracted from the simulation are expected to be in continuous form, as opposed to being in discretized form. Inputs and outputs from the simulation will be sampled data at the controller sampling period T .

The approach is to use the continuous models described earlier in combination with a Tustin transformation for integrators within the controller. By using this approach, the first-order model shown in figure 7 remains unchanged. The second-order model shown in figure 8 will have the integrator modified by the transformation

$$s^{-1} = \frac{T}{2} \frac{z+1}{z-1} \quad (47)$$

which is shown in figure 11. Combining this Tustin integrator with the second-order continuous model shown in figure 8 and expanding the controller portion of the closed-loop plant inversion model gives the NDI hybrid controller implementation shown in figure 12. This approach allows variables ω , ζ , and ω_n to be varied directly without the need for transformations. A state-space representation for the Tustin integrator is

$$\begin{aligned} x_{k+1} &= x_k + Tu_k \\ y_k &= x_k + \frac{T}{2}u_k \end{aligned} \quad (48)$$

A SOFFT hybrid controller implementation is illustrated in figure 13, where the filter implementation of equation (30) is used for the controlled variable(s). The only dynamics within this controller are for the discrete open-loop command model. In a simulation of this hybrid configuration, a Tustin model was found to be slightly better than the standard exponential discrete model because the desired output has a slight lead which helps to compensate for the first-order filter lag in the plant.

Simulation Results

Several of the configurations described in this paper were evaluated in MATRIXx BUILD by using a linear longitudinal plant model with four states and one control. The model was taken from the HARV

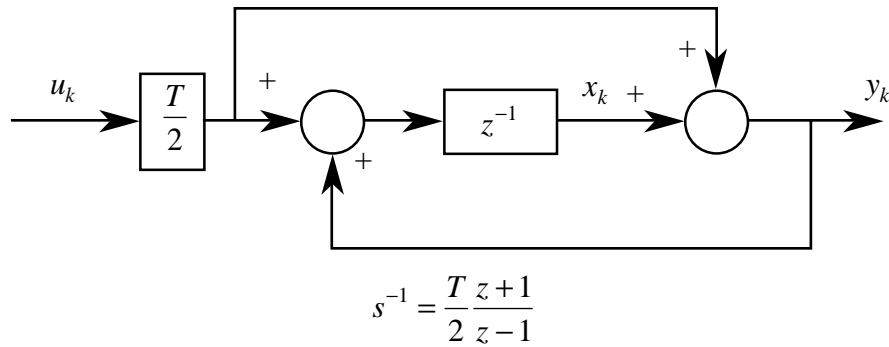


Figure 11. Tustin transformation for an integrator.

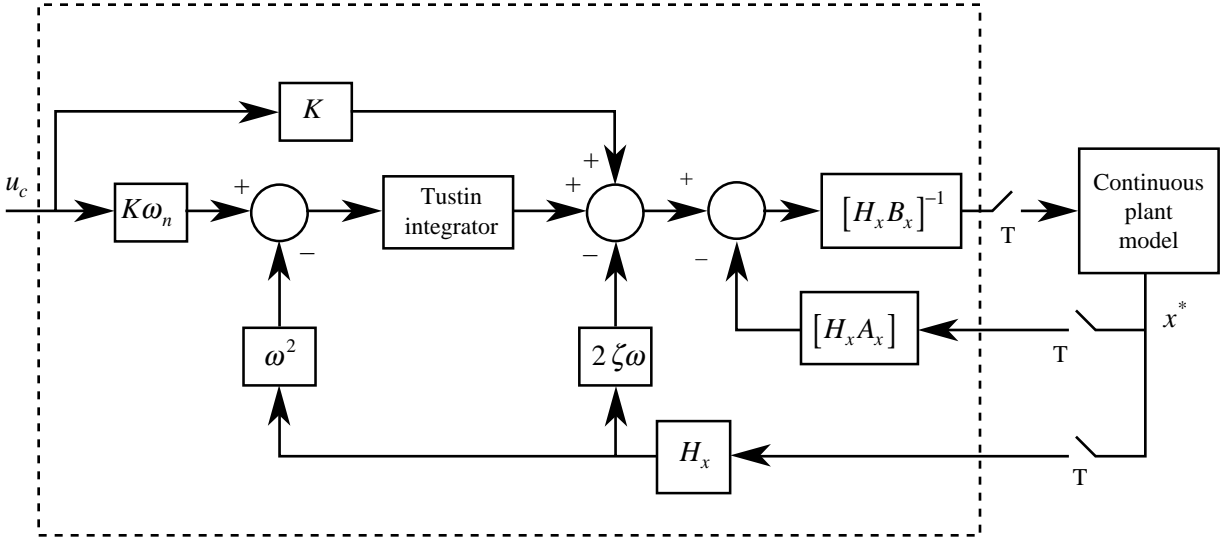


Figure 12. NDI hybrid controller implementation for a second-order continuous command model.

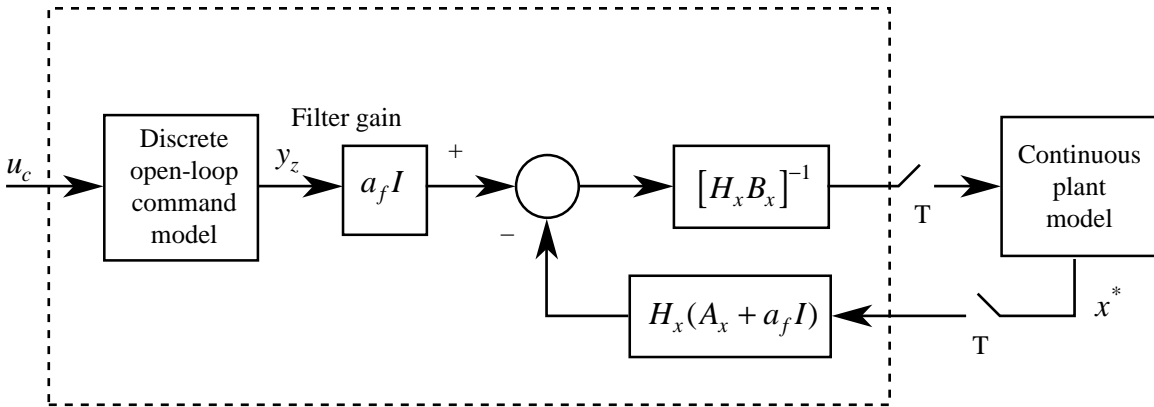


Figure 13. SOFFT hybrid controller implementation for including a filter in the controlled channel.

(High-Alpha Research Vehicle) database (ref. 9, see appendix for some longitudinal models) for a flight condition of Mach 0.7, $\alpha = 3.58^\circ$, and 25 000-ft altitude. The four states are velocity V , angle-of-attack α , pitch rate q and pitch attitude θ , and the control is a symmetric elevator.

A second-order command model was used for the response. Referencing equation (35), $\omega = 4$ rad/sec, $\zeta = 0.8$, $\omega_n = 1.5$ rad/sec, and $K = 10.667$ to give unity steady-state gain. A value of $\omega = 4$ rad/sec is level 1 (ref. 5) since the ratio of n_z / α is approximately 16 and the CAP (control anticipation parameter) is approximately 1.0, which is between the level 1 limits of 0.28 and 3.6. Also, $\zeta = 0.8$ is well above the minimum level 1 lower limit. The numerator zero was selected arbitrarily, but it is a reasonable number. A pitch-rate command was used giving H_x and H_y as shown in equation (24).

Configurations tested were

- 1) the standard SOFFT FF controller structure in figure 3

- 2) the equivalent SOFFT discrete FF controller structure in figure 4
- 3) the equivalent SOFFT continuous FF controller structure in figure 5
- 4) the NDI closed-loop continuous controller structure in figure 8
- 5) the NDI closed-loop discrete controller structure in figure 10
- 6) the NDI hybrid controller structure in figure 12
- 7) the SOFFT hybrid controller structure in figure 13

In each case a step input of unity gain and of two seconds duration was the forcing function, and a sampling period of 0.0125 seconds was used for the discrete structures. Based upon the parameter values selected, two seconds is sufficient to capture the response and settling time. The equivalent SOFFT discrete FF controller structure was used for the baseline test for these reasons: 1) a moment command M_{des} , was easily implemented, 2) an error signal for the difference between the command model response and plant model was readily available compared to the NDI formulations shown, and 3) it was discrete and was a very small change from the standard SOFFT configuration.

The first step was to verify that the equivalent SOFFT discrete FF controller configuration was correct by comparing it against the standard SOFFT FF controller structure in figure 3. All signals were identical and the error signal was zero. Simulation results for the baseline response are shown in figure 14. The left-hand column represents the four plant model outputs (V , α , q , θ), while the right-hand column contains the control signal $u_{x,k}^*$, the command model output $y_{z,k}$, the moment command M_{des} , and the error signal.

In figure 14, $u_{x,k}^*$ and M_{des} have nonzero values at time zero, which is due to the direct feedforward path from the input in figure 3. This result can also be seen in the equivalent SOFFT model in figure 4 since the plant inversion loop is driven by $y_{z,k+1}$. The step input was chosen at time zero to avoid numerical integration error. When the input was administered at a time greater than zero, the numerical integrator assumed the step to be a fast ramp between input points, leading to error in the continuous systems time responses (configurations 3 and 4). This anomaly was investigated, and the error was essentially eliminated by increasing the number of input data points by an order of magnitude. Inputting the step at time zero completely eliminated this problem.

The second step was to evaluate all seven configurations, as demonstrated by the pitch rate response in figure 15. Data for the first five configurations are identical to at least 5 digits. Both of the hybrid controllers have a sampling period of 0.0125 second, and these configurations both have some error in the time response. The pitch rate response of the NDI hybrid controller (sixth configuration) leads all other cases and has a slightly larger peak amplitude. This error is likely due to approximating the controller integrator by using a Tustin integrator (see fig. 12). The response of the SOFFT hybrid controller (seventh configuration) initially lags the response of the first five configurations, but it catches up by approximately 0.3 second. This configuration contains a Tustin open-loop command model and a filter frequency a_f of 160 rad/sec (see fig. 13). The filter frequency was selected to approximately balance the lead ($T/2$ sec) of the Tustin command model.

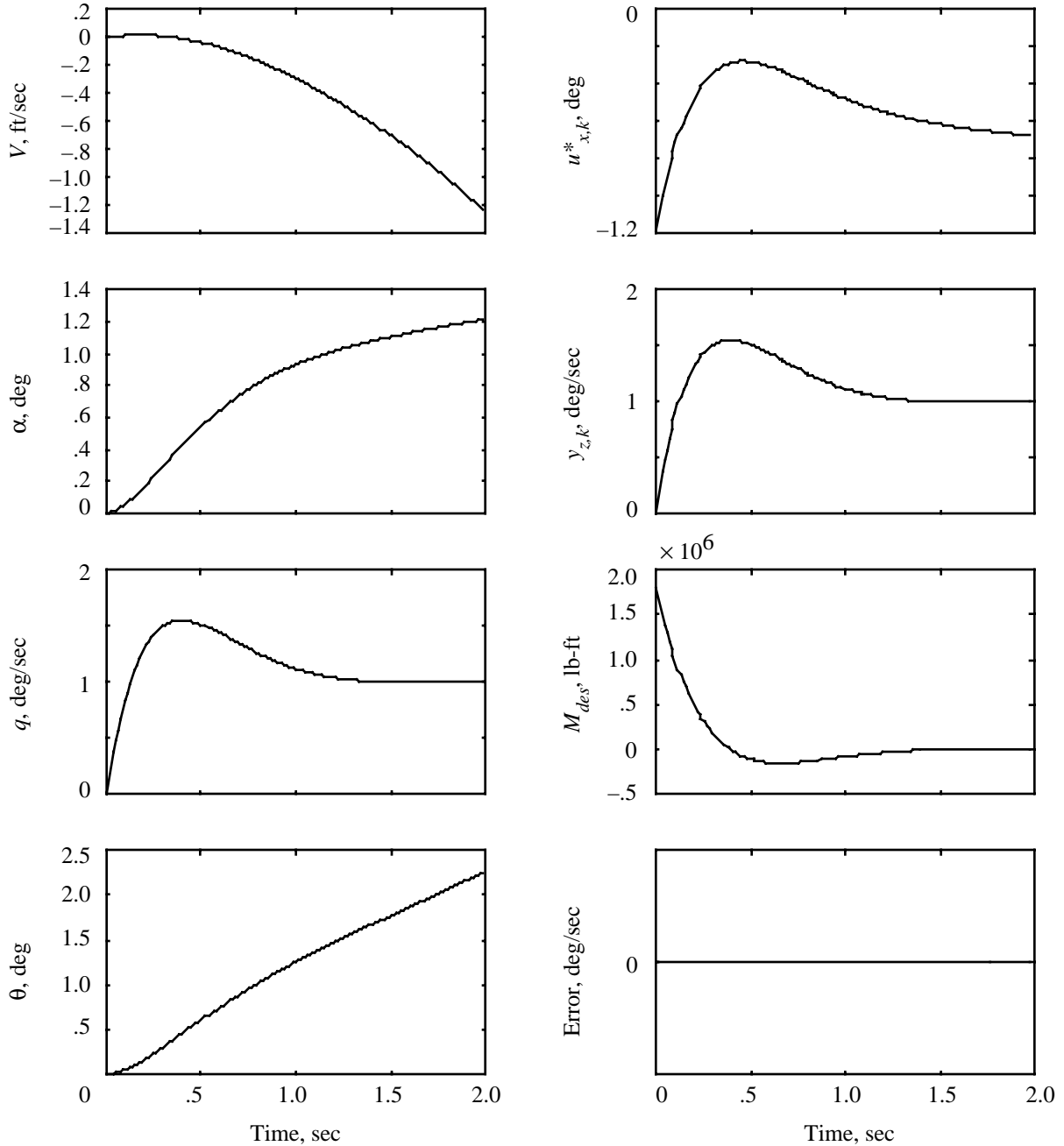


Figure 14. Baseline response for a two-second step input.

A second investigation was made to evaluate results with a control-signal position limiter of $\pm 0.8^\circ$ inserted prior to the plant model input. This limit was selected arbitrarily to limit the peak values of $u_{x,k}^*$. A doublet at u_c of unity magnitude and of one second full width was the forcing function. Figure 16 shows time history plots of the pitch rate response, the control signal into the limiter, and the control signal limiter output, which is also the plant input control. Three cases are shown:

1. the baseline case using the standard SOFFT FF controller structure in figure 3 with no limiting (solid line)

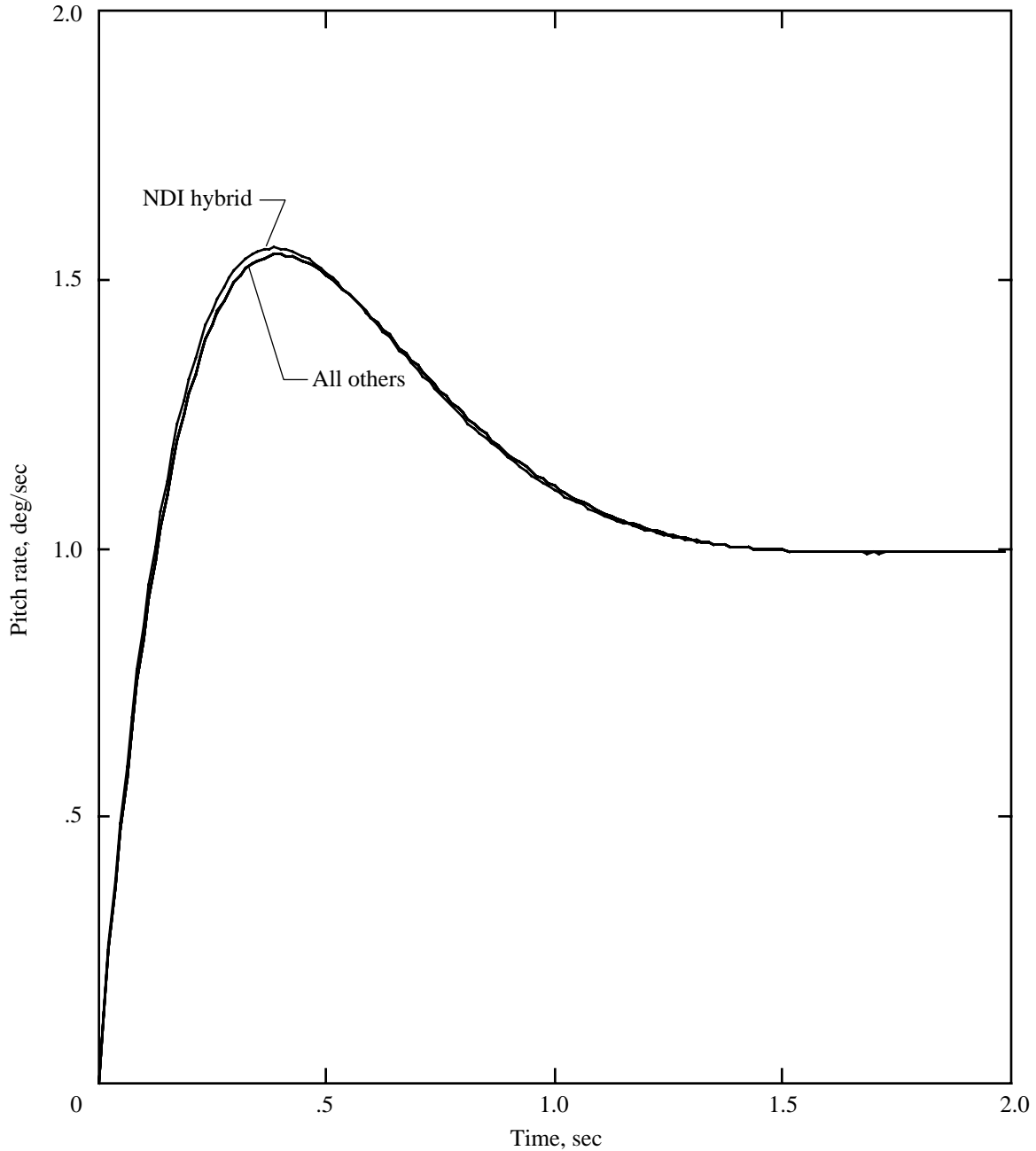


Figure 15. Pitch rate response for seven configurations.

2. the SOFFT hybrid controller structure in figure 13 with a limiter (dashed line)
3. the NDI hybrid controller structure in figure 12 with a limiter (dotted line)

Only two cases with control position limiters are shown since results for case 2 were very close to those of another SOFFT controller configuration with a limiter, and results for case 3 were very close to those of another NDI controller configuration with a limiter. In both cases, the hybrid configurations were slightly worse than their counterpart configurations.

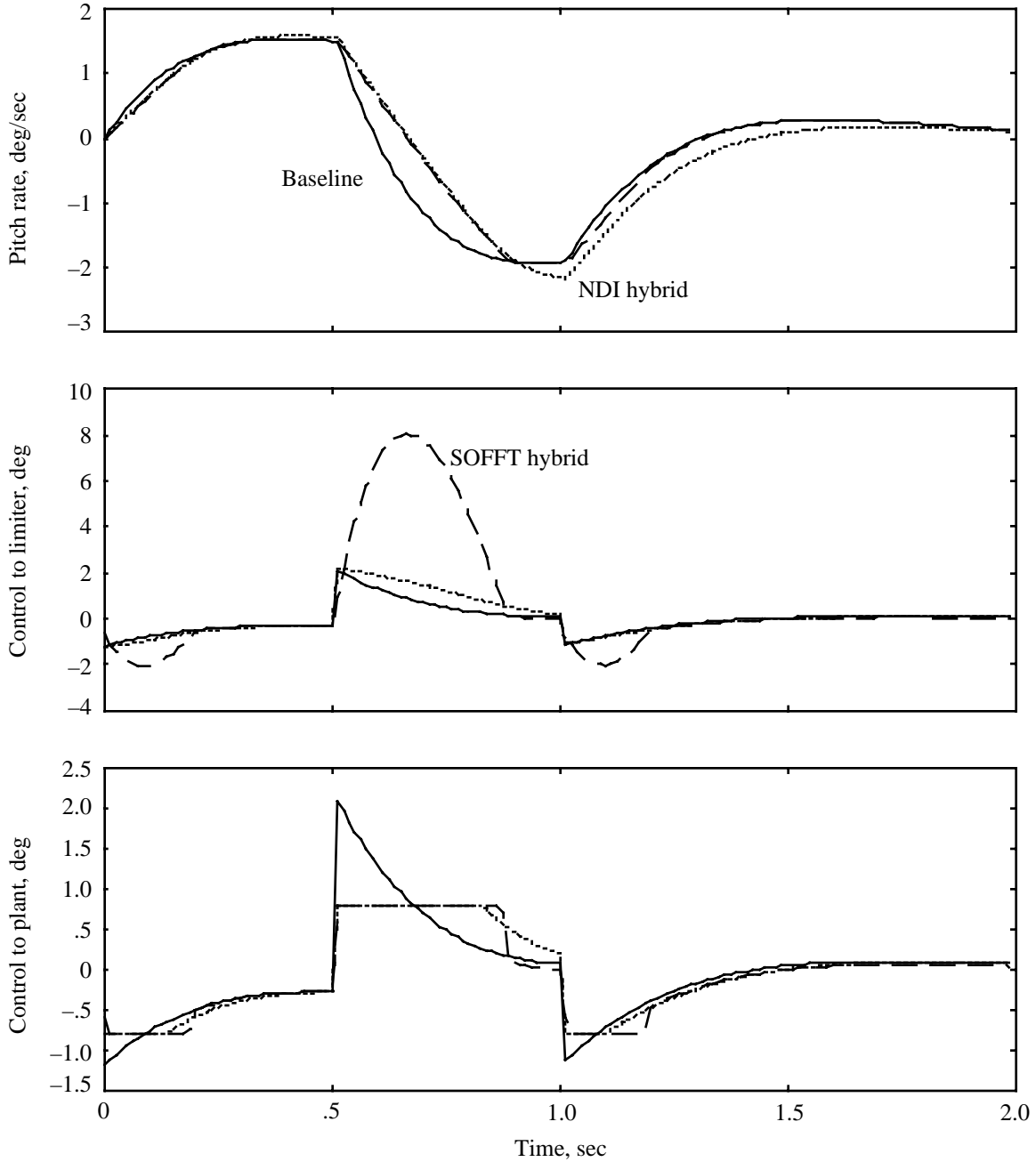


Figure 16. One-second duration doublet response for baseline and two hybrid configurations with actuator limiter.

Both hybrid controllers show approximately the same performance for the first 0.9 second, but then the NDI hybrid controller shows additional phase lag. Whenever the SOFFT hybrid control signal is not position-limited, the pitch-rate response matches the baseline response. The SOFFT hybrid control signal into the limiter has a significantly larger amplitude during saturation, but the control signal gets out of saturation much faster than the NDI hybrid control signal. These results could be misleading since the control signal of the SOFFT hybrid controller could possibly exceed a rate limit. Rate-limiting has not been investigated during this study, but it is important and will be investigated in the future.

A sinusoidal input of 0.5 Hz and 3 deg/sec amplitude at u_c was used to verify that the previous results are independent of a quick changing input. The amplitude was chosen such that the unlimited control signal would exceed the saturation limit of $\pm 0.8^\circ$ inserted prior to the plant model input, and the frequency was chosen since it is a reasonable pilot input and is within the bandwidth of the command model. Figure 17 has time history plots of the same signals shown in the previous example and the results are the same. Tracking performance of the controlled variable for the SOFFT hybrid configuration is better than that of the NDI hybrid configuration, but the control signal of the former case changes rapidly. If rate limiting is encountered, tracking performance would be reduced and additional problems would be encountered.

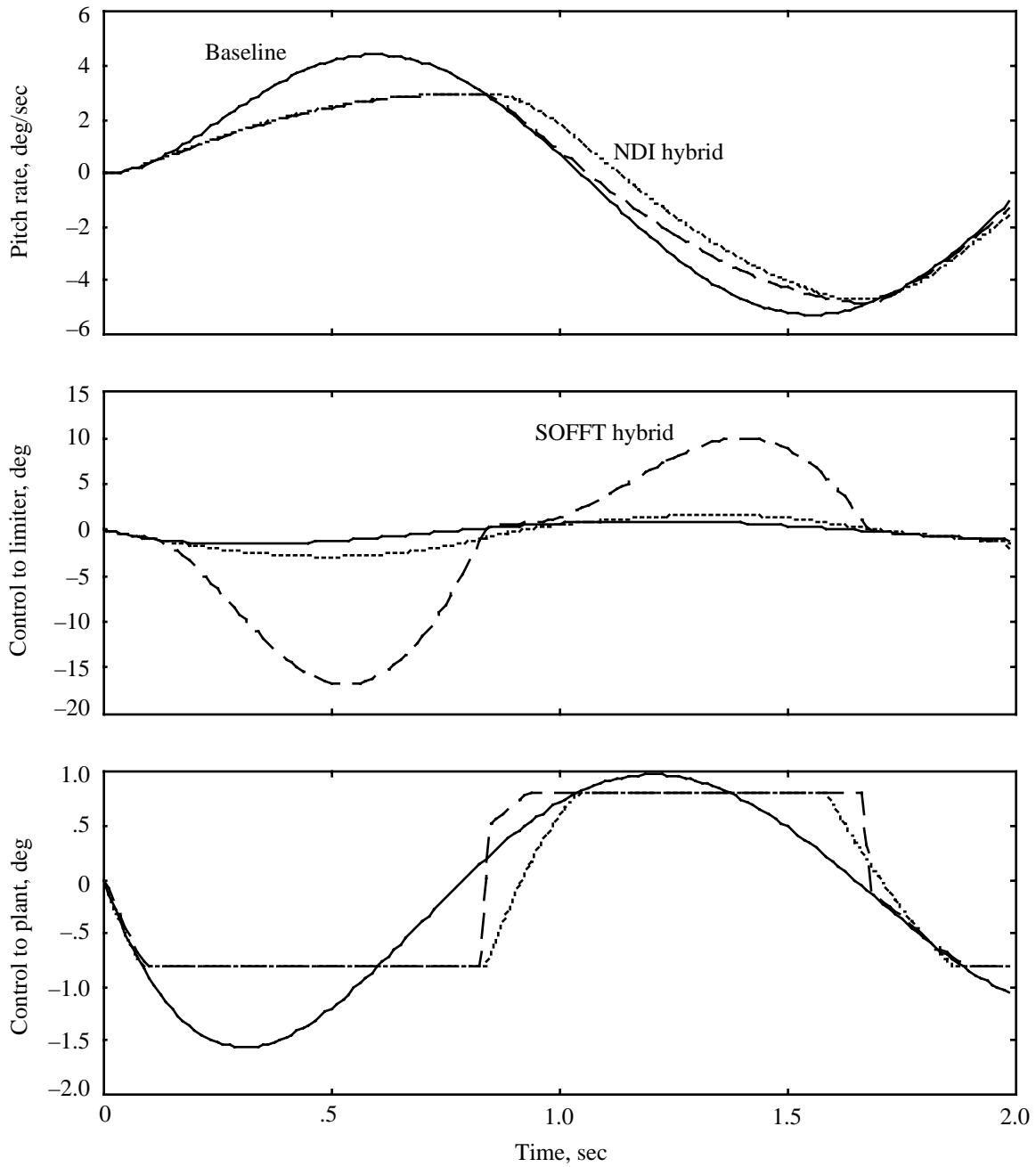


Figure 17. One-half Hz sinusoidal response for baseline and two hybrid configurations with actuator limiter.

Conclusions and Discussion

This paper contains the initial results of an ongoing study for developing a generic simulation tool to determine achievable control dynamics and control power requirements while undergoing simulation maneuvers with perfect tracking. The two approaches that were investigated were exact nonlinear dynamic inversion (NDI) and SOFFT (Stochastic Optimal Feedforward and Feedback Technology), and both continuous and discrete formulations were included for each approach. The following list contains the main conclusions and explanations where required:

1. Equations for SOFFT can be rearranged into a form that eliminates the need to explicitly calculate the feedforward gain matrices. The revised equations clearly illustrate a closed-loop plant model structure that performs plant inversion.
2. Equivalent models have been developed for both discrete and continuous versions of SOFFT. The original version of SOFFT had only been developed for a discrete model. Inertia terms can be incorporated into each of these configurations to create moment commands, and it can be seen that SOFFT and NDI have the same form for the closed-loop plant model.
3. The SOFFT approach uses an explicit open-loop command model whereas NDI integrates the command model into a closed-loop approach.
4. The transfer function for the controlled variable of the closed-loop plant model is an integrator for the continuous controller and a time delay for the discrete controller. Any linear combination of states can be used for the controlled variable. The internal dynamics for the uncontrolled states will be modified from the original open-loop characteristics. In addition, a nonminimum phase system will result in an unstable closed-loop system for any configuration since the zeros of the open-loop plant become poles of the closed-loop plant model.
5. First- and second-order models have been developed for continuous control systems, discrete control systems, and hybrid control systems. The NDI approach makes direct use of the transfer function characteristics of the plant inversion model in the controller characteristics and therefore uses one dynamic element less than the SOFFT controller.
6. Formulation of the discrete controller shows that the structure is the same as the continuous controller. The main difference is that gains for the discrete controller are combinations of terms used in the continuous controller. The discrete controller also requires an approximation of the discrete gains in order to implement in real time.
7. The typical situation for the application defined in this paper is to have a combination of a continuous plant and a sampled data controller that contains discrete dynamic elements, forming a hybrid control system. The plant will appear to be continuous since numerical integration will be used for the equations of motion and variables extracted from the simulation are expected to be in continuous form, as opposed to discretized form. Inputs and outputs from the simulation will be sampled data at the controller sampling period.
8. Seven control structure variations were evaluated in simulation by using a linear longitudinal model. As demonstrated by a two-second step input pitch-rate response, all configurations gave effectively the same results. The NDI hybrid controller has a slight error in the pitch rate response, which is likely due to approximating the controller integrator by using a Tustin integrator.

9. A control signal position-limiter was inserted at the plant input of both a SOFFT hybrid controller and an NDI hybrid controller. A pitch doublet and a sinusoid were used to test these configurations. The SOFFT hybrid controller gave better tracking performance in both cases, but the control signal changed rapidly when it came out of saturation, and it is possible that rate limiting, which would reduce performance, might be encountered. Rate limiting was not included in this ongoing study, but it is a source of concern.

The next major step in this study is to investigate use of a full nonlinear airplane simulation. A key aspect is to determine whether the desired variables can be extracted from the airplane aerodynamic database, which is typically in table form. The preferred approach is to extract aerodynamic moments (or moment increments) separately from control moments, as described in the first section on the review of NDI. If this approach cannot be accomplished, then the calculation of linear plant models for each iteration during a simulation will be investigated. Any of the configurations described in this paper can then be used with linear plant models.

References

1. Scott, Michael A.; Montgomery, Raymond C.; and Weston, Robert P.: Subsonic Maneuvering Effectiveness of High Performance Aircraft Which Employ Quasi-Static Shape Change Devices. *SPIE 5th Annual International Symposium on Smart Structures and Materials*, San Diego, USA, March 1-6, 1998.
2. Smith, P.R.: Functional Control Law Design Using Exact Non-Linear Dynamic Inversion. *AIAA Atmospheric Flight Mechanics Conference*, 94-3516-CP, pp. 481-486, August 1994.
3. Honeywell Technology Center; Lockheed Martin Skunk Works and Lockheed Martin Tactical Aircraft Systems: Application of Multivariable Control Theory to Aircraft Control Laws. WL-TR-96-3099, Final Report for March 1993 to March 1996, May 1996.
4. Gilbert, William P.; and Gatlin, Donald H.: Review of the NASA High-Alpha Technology Program. *High-Angle-of-Attack Technology*, Volume 1, Joseph R. Chambers, William P. Gilbert, and Luat T. Nguyen, eds., NASA CP-3149, Part 1, 1992, pp. 23-59.
5. Military Standard Flying Qualities of Piloted Aircraft. MIL-STD-1797A, Jan. 30, 1990.
6. Halyo, Nesim; Direskeneli, Haldun; and Taylor, Deborah B.: *A Stochastic Optimal Feedforward and Feedback Control Methodology for Superagility*. NASA CR 4471, November 1992.
7. Ostroff, Aaron J.; and Proffitt, Melissa S.: *Design and Evaluation of a Stochastic Optimal Feed-Forward and Feedback Technology (SOFFT) Flight Control Architecture*. NASA Technical Paper 3419, June 1994.
8. Roskam, Jan: *Airplane Flight Dynamics and Automatic Flight Controls, PART I*. Published by *Roskam Aviation and Engineering Corporation*, Ottawa, KS, 1979
9. Ostroff, Aaron J.; Hoffler, Keith D.; and Proffitt, Melissa S.: *High-Angle-of-Attack Research Vehicle (HARV) Longitudinal Controller: Design, Analyses, and Simulation*. NASA TP-3446, 1994.

REPORT DOCUMENTATION PAGE			Form Approved OMB No. 0704-0188	
Public reporting burden for this collection of information is estimated to average 1 hour per response, including the time for reviewing instructions, searching existing data sources, gathering and maintaining the data needed, and completing and reviewing the collection of information. Send comments regarding this burden estimate or any other aspect of this collection of information, including suggestions for reducing this burden, to Washington Headquarters Services, Directorate for Information Operations and Reports, 1215 Jefferson Davis Highway, Suite 1204, Arlington, VA 22202-4302, and to the Office of Management and Budget, Paperwork Reduction Project (0704-0188), Washington, DC 20503.				
1. AGENCY USE ONLY (Leave blank)		2. REPORT DATE August 1998	3. REPORT TYPE AND DATES COVERED Technical Memorandum	
4. TITLE AND SUBTITLE Study of a Simulation Tool To Determine Achievable Control Dynamics and Control Power Requirements With Perfect Tracking			5. FUNDING NUMBERS WU 522-21-61-01	
6. AUTHOR(S) Aaron J. Ostroff				
7. PERFORMING ORGANIZATION NAME(S) AND ADDRESS(ES) NASA Langley Research Center Hampton, VA 23681-2199			8. PERFORMING ORGANIZATION REPORT NUMBER L-17767	
9. SPONSORING/MONITORING AGENCY NAME(S) AND ADDRESS(ES) National Aeronautics and Space Administration Washington, DC 20546-0001			10. SPONSORING/MONITORING AGENCY REPORT NUMBER NASA TM-1998-208699	
11. SUPPLEMENTARY NOTES				
12a. DISTRIBUTION/AVAILABILITY STATEMENT Unclassified-Unlimited Subject Category 08 Distribution: Standard Availability: NASA CASI (301) 621-0390			12b. DISTRIBUTION CODE	
13. ABSTRACT (Maximum 200 words) This paper contains a study of two methods for use in a generic nonlinear simulation tool that could be used to determine achievable control dynamics and control power requirements while performing perfect tracking maneuvers over the entire flight envelope. The two methods are NDI (nonlinear dynamic inversion) and the SOFFT (Stochastic Optimal Feedforward and Feedback Technology) feedforward control structure. Equivalent discrete and continuous SOFFT feedforward controllers have been developed. These equivalent forms clearly show that the closed-loop plant model loop is a plant inversion and is the same as the NDI formulation. The main difference is that the NDI formulation has a closed-loop controller structure whereas SOFFT uses an open-loop command model. Continuous, discrete, and hybrid controller structures have been developed and integrated into the formulation. Linear simulation results show that seven different configurations all give essentially the same response, with the NDI hybrid being slightly different. The SOFFT controller gave better tracking performance compared to the NDI controller when a nonlinear saturation element was added. Future plans include evaluation using a nonlinear simulation.				
14. SUBJECT TERMS control, tracking, perfect tracking, dynamic inversion, NDI, SOFFT, achievable dynamics, continuous, discrete,			15. NUMBER OF PAGES 32	
			16. PRICE CODE A03	
17. SECURITY CLASSIFICATION OF REPORT Unclassified	18. SECURITY CLASSIFICATION OF THIS PAGE Unclassified	19. SECURITY CLASSIFICATION OF ABSTRACT Unclassified	20. LIMITATION OF ABSTRACT	